Updating HTDP for Two Recent Earthquakes in California

Chris Pearson and Richard Snay

ABSTRACT: This paper describes revisions to the Horizontal Time Dependent Positioning (HTDP) software carried out to address the motion associated with two recent California earthquakes. NOAA's National Geodetic Survey (NGS) developed HTDP to enable its users to compensate survey measurements for the differential movement associated with tectonic deformation, so that surveys conducted at different epochs may be compared. We focus on the process of selecting and validating models for two recent earthquakes in California, prior to their inclusion in version 2.9 of this software (HTDP v2.9)—the Parkfield earthquake with a magnitude of 6.0, which occurred on September 28, 2004, and the San Simeon, California earthquake with a magnitude of 6.5, occurring on December 22, 2003. The process of modeling and correcting for deformation can be well illustrated by utilizing data collected in the vicinity of these earthquakes, because they represent contrasting styles of deformation—Parkfield exhibited strike-slip motion and San Simeon was predominantly a blind-thrust earthquake. Also, while both earthquakes were relatively small, they produced significant displacements (though restricted to a relatively small area in central California). The Parkfield earthquake, in particular, produced an unusually high proportion of post-seismic deformation. This deformation can accumulate during a period of a few months after the earthquake, whereas co-seismic deformation occurs suddenly during an earthquake. Quantifying and characterizing deformation at these disparate time scales represents a major challenge to developing the accurate models of deformation that are required to support modern, high-accuracy surveying in tectonically active areas such as California. This study also confirms the importance of including separate dislocation models of the co-seismic and post-seismic deformation, because, as was the case for Parkfield, post-seismic deformation can be comparable in magnitude to co-seismic deformation.

KEYWORDS: Horizontal Time Dependent Positioning, HTDP, tectonic plate, co-seismic deformation, post-seismic deformation, differential movement, earthquake, California

Introduction

Since the 1960s, geologists have known that the surface of the Earth is partitioned into a series of tectonic plates that are in constant motion relative to each other at rates which are typically about several centimeters per year. These plates generally move as rigid blocks; however, at their edges there is a zone (often called a plate boundary) where they move against each other, causing such geologic phenomena as earthquakes. The contiguous United States straddles two tectonic plates. The North American Plate contains all of the contiguous states, except for a small part of western California which resides on the Pacific Plate. The plate boundary zone between these two plates passes offshore, north of San Francisco, and continues northward slightly offshore along the Pacific coast. As a result of its proximity to this plate boundary, a zone—a few hundred km wide and including most of California, Nevada, Oregon Washington and Alaska—is deforming. This deformation causes the relative position of points on the Earth to change with time. Consequently, survey measurements taken at different times will differ, and we must have a method to compensate for this change, or else the resulting coordinates will be systematically in error.

In the ITRF and WGS 84 reference frames, all points on both the Pacific and North American plates have nonzero velocities (Snay and Soler 2000). The NAD 83 reference frame, however, is defined so that all points on the North American Plate located away from this plate boundary zone will have (on average) zero horizontal velocities. Points located within the Pacific–North American plate boundary zone will have NAD 83 velocities that are transitional between the respective velocities of these two plates and, as a result, have

Chris Pearson, National Geodetic Survey, 2300 South Dirksen Pkwy, Springfield, IL 62703. E-mail: <Christopher.Pearson@illinois.gov>. **Richard Snay,** National Geodetic Survey 1315 East West Highway Silver Spring, MD 20910.

nonzero NAD 83 velocities with magnitudes of up to 5 cm/yr. Accurate surveying in the western U.S. requires a model describing crustal velocities and earthquakes so that survey measurements can be corrected for differential movement and surveys conducted at different epochs may be compared. NOAA's National Geodetic Survey (NGS) has developed the HTDP (Horizontal Time Dependent Positioning) software that enables its user to make these corrections (Snay 1999).

The deformation modeled by HTDP is caused by the junction of two tectonic plates moving in different directions, and it is accommodated by geologic faults that extend from the surface to points deep within the crust of the Earth. The crust, however, is comprised of two layers that deform in quite different ways. These layers are separated by a broad zone called the brittle–ductile transition zone. In the top layer (known as the brittle region) rocks deform following the same elastic principles as ordinary engineering materials. Here deformation causes increasing stresses that eventually exceed the frictional strength of the faults leading to an earthquake. Deeper in the crust, where conditions are hotter, the rocks behave in a ductile manner. Here deformation occurs by a slow continuous process, and stresses never reach a value sufficient to cause catastrophic failure. As a result, two quite different processes are responsible for the deformation in the western states.

The first of these, known as the secular field, represents the slow response of the deeper part of the crust to the differential movement of the two tectonic plates. Faults in the lower crust accommodate this motion by sliding stably without earthquakes, and this deformation is transmitted through the elastic crust to the surface. While the resulting secular velocities are fairly small, up to about 5 cm/yr in some places, the effect accumulates with time and is large enough that it cannot be ignored. The secular velocities are thought to be relatively constant, such that once this field is mapped, it need not be changed, although periodic updates may be needed to reflect our growing knowledge of crustal dynamics.

The second process is deformation associated with earthquakes which results when the stress—caused by the elastic strain associated with the secular velocity field—exceeds the frictional force on the fault that resists sliding. In this case, the fault will suddenly slip, and quite large displacements can happen within a period of few minutes or less. The co-seismic portion of the deformation field is therefore different because earthquakes happen in an unpredictable way, and each time there is a new earthquake, the HTDP software must be updated to address the associated deformation.

Because these two processes are very different, both temporally and spatially, two quite different methodologies are required to correct for them. The secular field is represented by an interpolation scheme of the velocity field that provides an estimate of the velocity difference between any two points within the plate boundary zone, while earthquakes are represented using dislocation models (Okada 1985; Savage 1980) that define the slip on related geologic faults.

This paper describes the NGS process for modeling earthquakes, focusing on two recent earthquakes in California (Figure 1), which were the largest to occur in the contiguous United States since 2000. Characterizations of the co- and post-seismic motion of these earthquakes were included in HTDP V 2.9 released in January 2007. Updating HTDP was a necessary component for the incorporation of GPS observations made before and after the earthquakes into the recent nationwide adjustment undertaken by NGS to create a new realization of the NAD 83 reference system (Pearson 2005; Vorhauer 2007).

Displacements Associated with Earthquakes

The deformation associated with an earthquake is caused by a fault or fracture in the Earth that slips suddenly due to the stress in the surrounding rocks. Sometimes the break extends to the surface, in which case the displacement will change very suddenly as one side of the fault will move one way while the opposite side moves in the opposite direction. More commonly, though, the break does not reach the surface. Even in this case, the earthquake will cause surface displacements because a slip on the fault will cause sympathetic movement in the surrounding rocks, and this deformation will propagate through the Earth to the surface.

A slip on the fault also has the effect of allowing the material surrounding the fault to rebound as the elastic strain in the surrounding rocks (caused by deformation associated with the secular velocity field) is released. This releases the elastic strain in the rocks surrounding the epicentral region, resulting in the deformation associated with the earthquakes and extending a

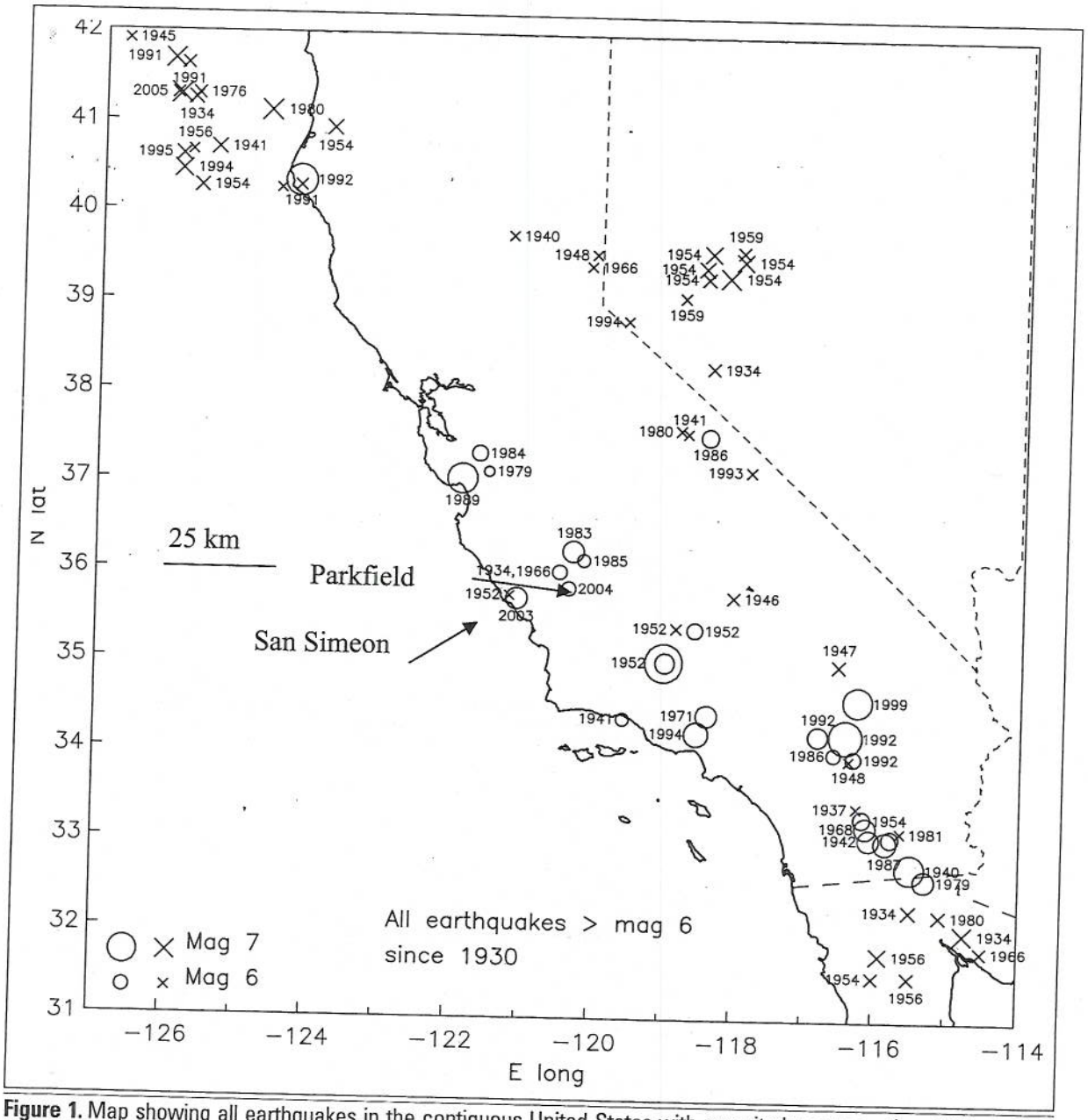

Figure 1. Map showing all earthquakes in the contiguous United States with magnitudes greater than 6. Those that have models included in HTDP v2.9 are identified by circles; those that do not are identified by an "x." Arrows identify locations of the Parkfield and San Simeon earthquakes.

considerable distance from the fault. In large earthquakes, measurable displacement can extend hundreds of kilometers from the earthquake. The deformation that occurs within the first few minutes of an earthquake occurrence is called co-seismic deformation.

In small earthquakes, where the material near the fault is cool enough to be fully solid, the deformation associated with an earthquake will be completed within a few minutes, and co-seismic deformation is all that will occur. In large earthquakes, however, the rupture may extend deep enough, so that the bottom of the active part of the fault is near the brittle–ductile transition. The adjacent ductile parts of the crust will respond to the stress caused by the earthquake and the resulting deformation is much slower, typically lasting for several months or years. This slow deformation is not associated with noticeable seismic waves or shaking and is called post-seismic deformation.

The final deformation field associated with the earthquake is the sum of the co-seismic and post-seismic components. Figure 2 shows co-seismic

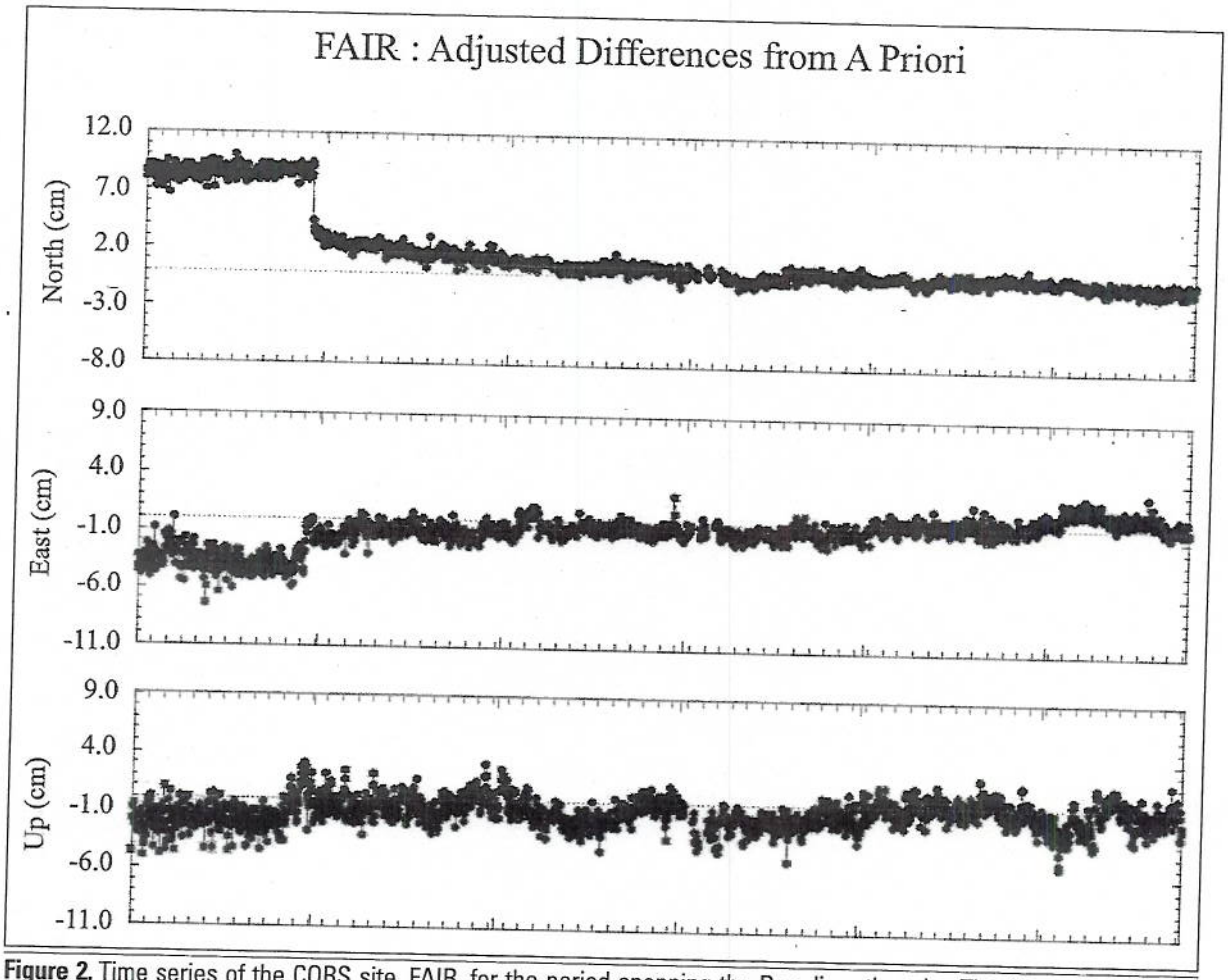

Figure 2. Time series of the CORS site, FAIR, for the period spanning the Denali earthquake. The time axis starts on December 2, 2001; day-of-year 336, or the first day when ITRF00 became operational. Each major division includes 1 year of data while the minor ticks represent 30 days. The Denali earthquake occurred near the end of the first year of the time interval. Figure shows both a sudden co-seismic displacement and the more gradual exponential decay of the post-seismic slip.

and post-seismic deformations for the continuously operating reference station FAIR during a time period including the 2002 Denali Earthquake which was the largest earthquake to occur within the United States since the establishment of the CORS network.

HTDP v2.9 contains models for 28 earthquakes which have been developed from measured deformation on the Earth's surface (e.g., Segall and Davis 1997; Murray and Langbein 2006). The locations of these earthquakes range from Alaska to the Mexican border, although all but one occurred in California. The two most recent are the magnitude 6.0 Parkfield earthquake that occurred on September 28, 2004, and the magnitude 6.6 San Simeon earthquake that occurred on December, 22. 2003, about 60 km west of the epicenter of the Parkfield earthquake. All 28 earthquakes are listed in Table 1, and their locations are plotted in Figure 1.

Dislocation Models

Predicting the effect of an earthquake on positional coordinates utilizes the relatively simple mathematical equations provided by dislocation theory (Okada 1985; Savage 1980). The equations predict the elastic response of a uniform half-space to slip on a rectangular patch embedded in the half-space. Each dislocation represents a rectangular patch in the Earth where one side slips relative to the other by a uniform amount. The term "dislocation" is used because the slip displacement is uniform over the rectangle, thereby producing a discontinuity along the

Earthquake	Date	Magnitude	# dislocations
Parkfield	1934	6	98
El Centro	1940	6.7	5
Red Mountain	1941	5.9	1
San Jacinto	1942	6.5	1
Kern County	1952	7.7	3
San Jacinto	1954	6.2	1
Prince Wm. Sound, AK	1964	9.2	68
Parkfield	1966	5.6	98
Borrego Mtn.	1968	6.4	1
San Fernando	1971	6.4	4
Imperial Valley	1979	6.6	1
Coyote Lake	1979	5.9	1
Homestead Valley	1979	5.6	1
Coalinga	1983	6.5	1
Morgan Hill	1984	6.2	1
Kettleman Hills	1985	6.1	1
Chalfant Valley	1986	6.5	2
North Palm Springs	1986	6	1
Superstition Hill	1987	6.6	2
Whittier Narrows	1987	6	1
Loma Prieta	1989	7.1	1
Petrolia	1992	7.1	1
Landers/Big Bear	1992	7.3	26
Joshua Tree	1992	6.1	19
Northridge	1994	6.6	1
Hector Mine, California	1999	7.1	75
San Simeon	2003	6.5	200
Parkfield	2004	6	300

Table 1. List of earthquakes having models in HTDP v2.9.

edges of the patch. The model is shown conceptually in Figure 3.

A dislocation model is obviously very similar to what happens during an earthquake where one side of the fault slips relative to the other. A single dislocation can model an earthquake. However, the requirements that the slip is uniform and that the slipped region is shaped like a rectangle represent serious limitations because real earthquakes are much more complex. These difficulties are overcome by partitioning the fault into a series of small rectangular dislocations which, taken together, better approximate the complexity associated with a real earthquake. In the earthquakes discussed here, as many as 200 dislocations were required to map each earthquake.

Dislocations are determined by varying the properties of the dislocations such as the amount of slip and the geometry of the rectangular patch until the predictions of the dislocation models provide a satisfactory match with observations made during and after an earthquake. There are two main types of observations that are used to constrain dislocation models—surface measurements of displacements obtained using the Global Positioning System (GPS), which may be augmented with InSAR (Interferometric Synthetic Aperture Radar) data (Burgmann et al. 2000), and seismic-wave data generated by an earthquake.

Post-seismic Slip

Along with the very sudden co-seismic displacements, earthquakes can be followed by slow displacements which decay for a few months (Freed 2005). This motion is called post-seismic slip. Post-seismic slips are important to surveyors because they contribute to the total deformation field on the surface that will affect the relative position of points causing them to change from the relationships measured during earlier surveys. The models for the two earthquakes discussed in this paper assume that the decay of post-seismic slip follows an exponential equation, although others (i.e., Freed 2007; Langbein et al. 2006) suggest that a logarithmic equation might be more appropriate. In the exponential function, the postseismic slip ($s_{ps}(t)$) at any given time after the earthquake is represented by the equation:

$$s_{ps}(t) = A_{ps}(1 - e^{-t/\tau}) \qquad (1)$$

where:

A_{ps} = the total post-seismic slip on the rectangular patch;

t = the amount of time that has elapsed since the earthquake (that is, the amount of time between the earthquake and the date in question); and

τ = the decay time constant.

Because the decay time constant for the Parkfield earthquake has a value of 32 days (Johanson et al. 2006), the exponential expression in Equation

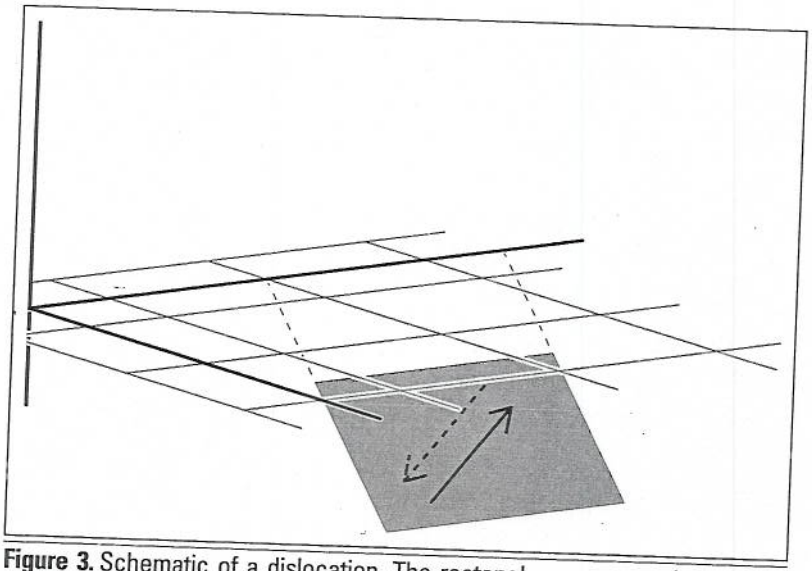

Figure 3. Schematic of a dislocation. The rectangle represents the slipping patch of the fault. Arrows represent the shear applied on the edge of the dislocation, and the horizontal line above the rectangle represents the surface of the Earth.

(1) rapidly approaches 1 in value, and the post-seismic slip distribution approaches the values of the post-seismic dislocation coefficients (A_{ps}). The values of $s_{ps}(t)$ for a unit value of A_{ps} are plotted as a function of t in Figure 4. Note that if 100 days or more have elapsed since the earthquake, the slip on the fault is, for all intents and purposes, equal to the coefficient A_{ps}.

Figure 4 also demonstrates the logarithmic relationship of Freed (2007). The logarithmic and exponential relationships agree over the first 100 days or so, but then the logarithmic relationship predicts higher displacements. For the purposes of this study, we prefer the exponential function for two reasons; first, because the ever-growing nature of the log function will produce unrealistically large displacements when extrapolated to long time periods, thus making it inappropriate for the purpose of correcting survey measurements which may be taken many years after the earthquake. The second reason is that quantitative models allowing us to predict the post-seismic deformation as a function are only available as coefficients of an exponential power law (e.g., as in Equation (1)).

The Parkfield Earthquake

The magnitude 6.0 Parkfield earthquake occurred on 28 September 2004 at 10:15 a.m. Pa-

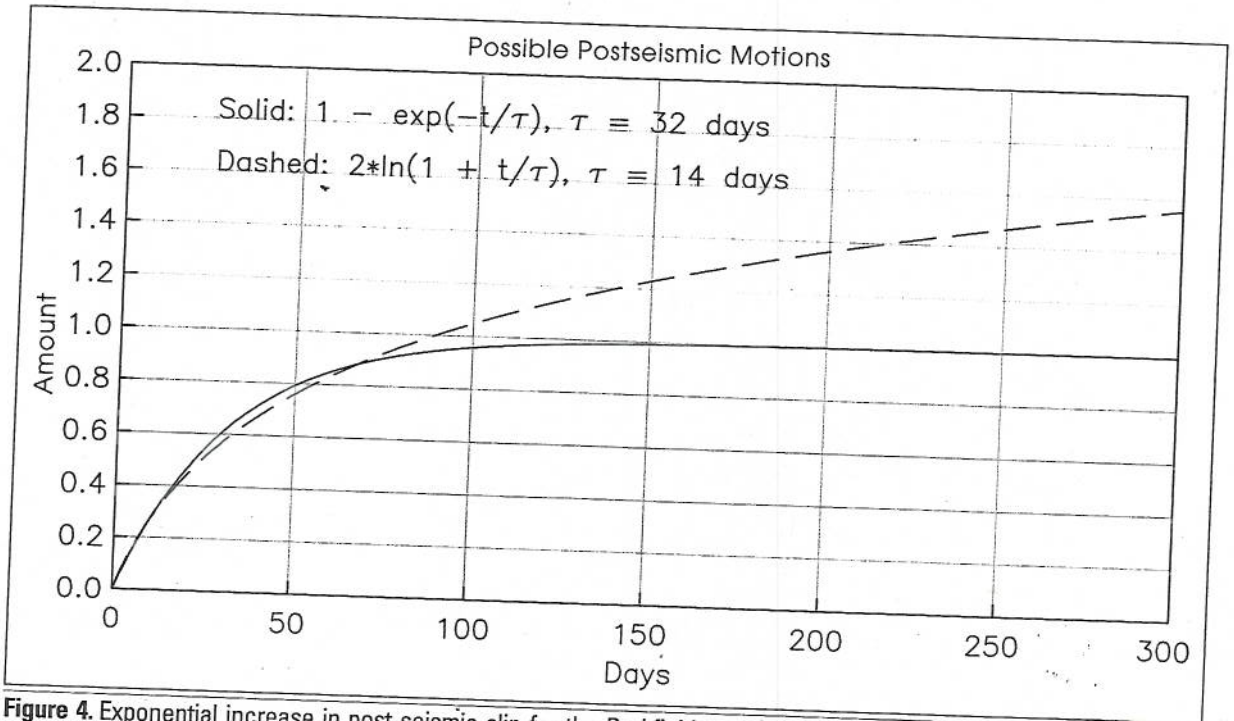

Figure 4. Exponential increase in post-seismic slip for the Parkfield earthquake, for the exponential decay shown in Equation (1) and the logarithmic equation of Freed (2007).

cific Daylight Time near the small town of Parkfield, California. It was a strike-slip earthquake on the San Andreas Fault. Maximum displacement vectors for this earthquake were generally less than 0.1 m but, because this was a strike-slip event where vectors on opposite sides of the fault point in opposite directions, which would result in up to 0.2 m of relative motion on GPS baselines or other survey measurements that cross this fault (see Figure 8 of Johanson et al. 2006).

This earthquake was very unusual in that the post-seismic deformation around the fault was comparable in magnitude to the co-seismic movement. For this reason, it is essential that both co-seismic and post-seismic motion be included in our model; neglecting the post-seismic component of the deformation would cause the corrections applied to survey data to be significantly underestimated.

Because of the large post-seismic displacement associated with this earthquake, we used two dislocation models—one for the co-seismic deformation and another for the post-seismic deformation. Both models were provided by Johanson et al. (2006). They were constrained by surface deformation measurements (both GPS and InSAR data) without using seismic body waves. The parameters of the post-seismic dislocation model are different from the co-seismic model because they represent coefficients of the post-seismic "slip."

These coefficients are amplitudes of an exponential function describing decaying slip rather than estimates of a slip on the fault plane (s_{ps}) that are representative of any particular time. They must be multiplied by a function of time as in Equation (1) to provide a model that can be used to predict the deformation at a given time. However, as shown in Figure 4, the exponential function in Equation (1) rapidly approaches 1 in value once the elapsed time since the earthquake exceeds a value about three times the characteristic time, which Johanson et al. (2006) determined to be 32 days for this earthquake. Thus, when at least 100 days have elapsed, the post-seismic deformation is essentially complete and the post-seismic dislocation coefficients can be treated as a dislocation model which will predict the total post-seismic deformation field.

Because HTDP currently lacks the ability to predict the slow accumulation of post-seismic deformation after an earthquake, we combined the co- and post-seismic dislocations into a single model which predicts the total (co- and post-seismic) deformation associated with the earthquake, but which does not follow the gradual development of the post-seismic displacement in the first few months after the earthquake because the post-seismic component is modeled as if it occurred instantaneously.

San Simeon Earthquake

The San Simeon earthquake occurred on December 22, 2003, within the coastal ranges of central California, about 60 km west of the epicenter of the Parkfield earthquake. The earthquake had a magnitude (Mw) of 6.6 and was significantly larger than the Parkfield earthquake. While the earthquakes occurred in relatively close proximity, in some ways they could not be more differ-

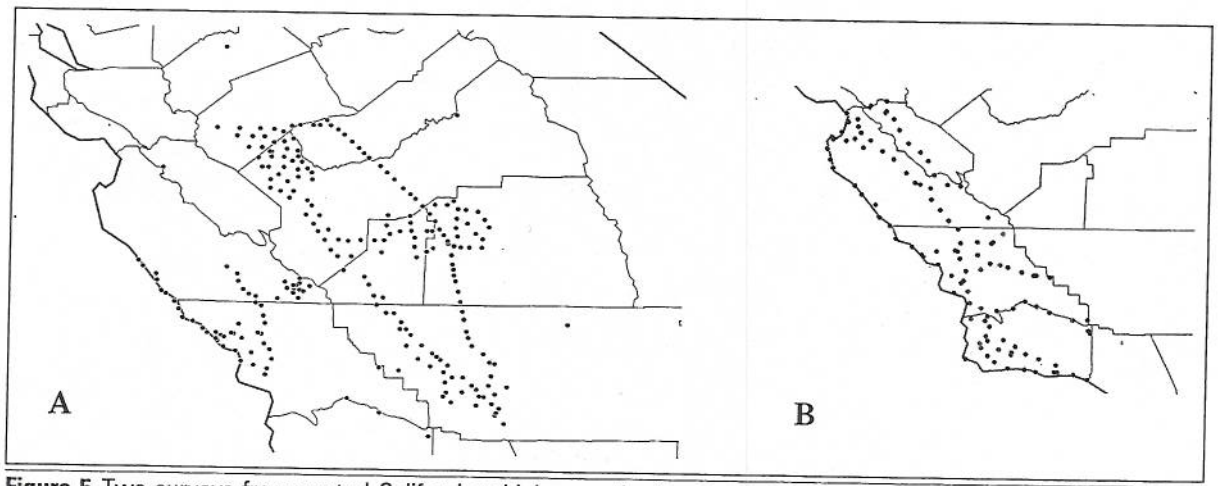

Figure 5. Two surveys from central California which span the hypocentral region of the Parkfield and San Simeon earthquakes. Project GPS 716 (labeled A) took place in 1993, over 10 years before the two earthquakes, and project GPS 2107 (labeled B) was carried out in 2004, after the San Simeon earthquake.

ent. In contrast to the Parkfield earthquake, which was a strike slip earthquake, the San Simeon earthquake was a blind thrust event, which means that the two sides of the inclined fault plane moved toward each other. Because this was a blind thrust, the fault plane did not reach the Earth's surface. As a result, even though the San Simeon earthquake was larger that the Parkfield earthquake, the surface displacement vectors are smaller, but they were spread over a larger area.

For this earthquake we tried dislocation models from two sources. The first model, developed by Ji et al. (2004), was developed primarily by inverting seismic body waves augmented with a small number of displacements measured at Continuous GPS (CORS) stations, all of which were located to the northeast of the epicenter. As a result, the model provided limited constraints on the surface deformation field, particularly near the epicenter. In addition, these data provided insufficient information to allow an estimate of the post-seismic motion to be developed because post-seismic slip does not produce seismic waves. Later, Johanson et al. (2006) developed a second model for this earthquake.

As with the Parkfield earthquake, the models were constrained by surface deformation measurements (both GPS and INSAR data) without using seismic body waves. This study also produced a model of the post-seismic slip similar to the Parkfield study discussed above. We again combined the co- and post-seismic dislocations into a single model that predicts the total (co- and post-seismic) deformation associated with the earthquake. While the models are quite similar, we prefer the Johanson (2006) model due to the fact that it was constrained by much more detailed measurements of the surface deformation field and because post-seismic deformation, which can be estimated only from this study, added a small but still measurable contribution to the total deformation associated with the earthquake.

Effect of the HTDP Update on the National Adjustment

Horizontal Time Dependent Positioning fills a critical role in facilitating the success of the Na-

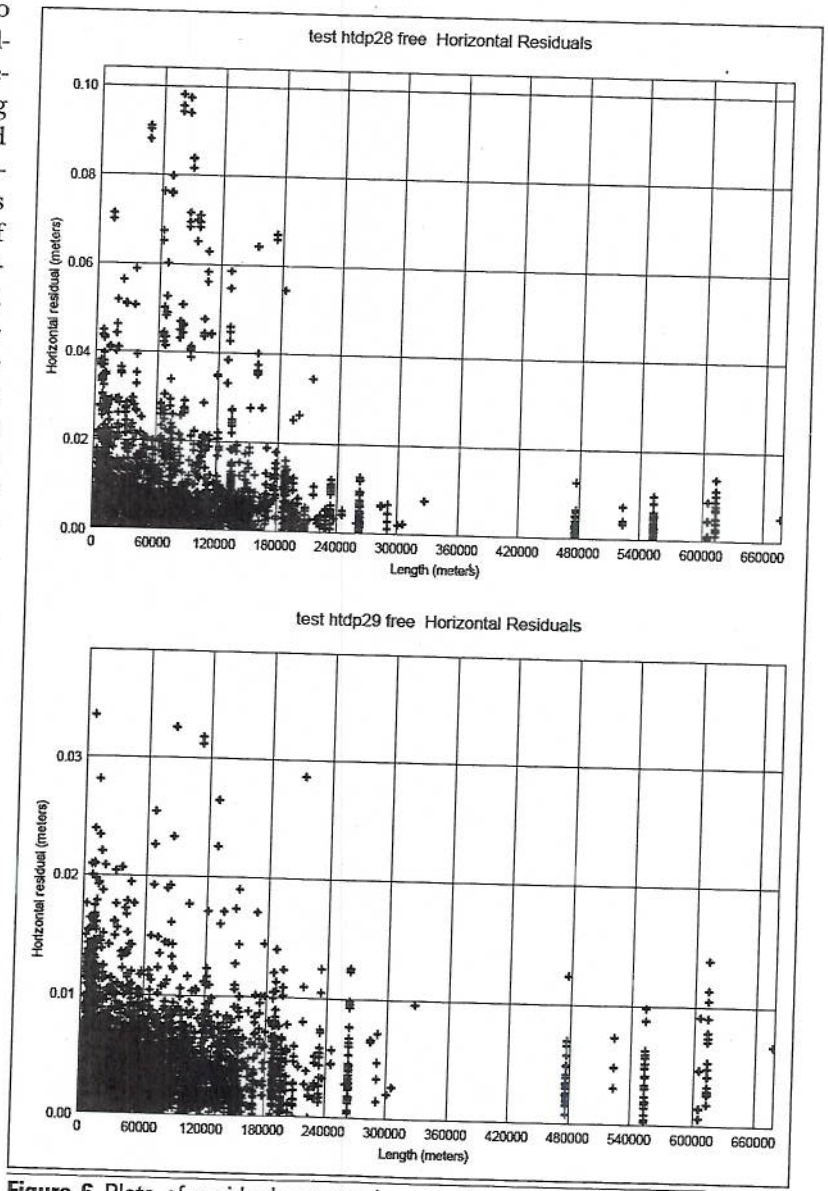

Figure 6. Plots of residuals versus baseline length for differential GPS observations from each adjustment of two surveys performed in central California, which span the hypocentral region of the Parkfield and San Simeon earthquakes. The top residual plot was developed using HTDP v2.8, which lacks models of the Parkfield and San Simeon earthquakes to "correct" the survey observations, while the lower one used HTDP v2.9, which includes models of the Parkfield and San Simeon earthquakes.

tional Adjustment of 2007 (Pearson 2005; Vorhauer 2007) because the GPS baselines being adjusted were collected over 15 years ago and some mechanism for estimating and correcting for the effects of crustal deformation must be utilized. If not, the deformation that has not been modeled will cause vectors measured at different times to not fit. The importance of having a correct model of crustal deformation while adjusting survey measurements in tectonically active areas cannot be overemphasized.

In order to demonstrate the effects that proper earthquake models can have on the adjustment of survey data in tectonically active areas, we performed two adjustments of a pair of surveys in California which span the hypocentral region for the Parkfield and San Simeon earthquakes. The first adjustment used HTDP v2.8 which lacks models for the Parkfield and San Simeon earthquakes; the second adjustment used HTDP v2.9 which includes such models. One of the two surveys, referred to as GPS 716, was conducted in 1993 by NOAA's National Geodetic Survey over a period of 10 years before the two earthquakes occurred; the second survey, referred to as GPS 2107, was conducted in 2004 by the California Department of Transportation, after the San Simeon earthquake. Figure 5 shows the extent of the two surveys and Figure 6 shows residuals for the two adjustments. Including models of the Parkfield and San Simeon earthquakes reduced the maximum residuals by a factor of 3.

Future Plans

A new model of the secular velocity field is being determined, and it will be incorporated into the HTDP software in 2008. This model is based on DEFNODE software developed by McCaffrey (2004). As part of this process, an analytical model representing horizontal crustal motion in the western contiguous states of the U.S. is being developed, which will incorporate all the major active faults in the region into a single model building on studies by Becker et al. (2005), Meade and Hager (2005), McCaffrey (2005), and McCaffrey et al. (2007). This new comprehensive model will be checked every year or so against all stations with well determined velocity vectors, and any residual differences between the model vectors and the latest observed vectors will be modeled separately for the purpose of updating HTDP. For HTDP users, the result will provide a significantly more accurate model of crustal deformation in the western United States. In the future, we also hope to expand the geographic scope of HTDP to include Alaska and the western coast of Canada.

Conclusions

The HTDP software has been updated to include dislocation models for the San Simeon and Parkfield earthquakes, the two largest earthquakes to occur in California since 2000. The revised software has been released as HTDP v2.9. Including the models of these two earthquakes has significantly improved the ability to correct historical surveying measurements impacted by crustal motion in central California.

The growing use of seismic body waves as a constraint for dislocation modeling provides challenges to organizations such as NGS which use dislocation models to estimate surface deformation fields for the purpose of correcting for crustal motion between surveys of different periods. This is because, unless significant constraints from surface deformation measurements are included, the model will not faithfully replicate surface displacements. In addition, dislocation models, derived solely from seismic body waves, include only the co-seismic portion of the earthquake slip, but the earthquakes examined in this paper—particularly the Parkfield earthquake—show that post-seismic slip on a fault can significantly add to the total earthquake-related deformation. The models we included were both derived from GPS vectors and InSAR measurements which directly measure surface deformation. They also both contained explicit models of post-seismic deformation.

ACKNOWLEDGMENTS

We thank Ingrid Johanson of the U.S. Geological Survey and Roland Bürgmann of the University of California, Berkeley, for generously providing advice and sharing unpublished results in developing the dislocation for the San Simeon earthquake. Dale Pursell provided the residual plots shown in Figure 6. This paper benefited from reviews by Marti Ikehara, Dru Smith, and Dave Minkle of NOAA's National Geodetic Survey and two anonymous reviewers.

REFERENCES

Becker, T., W.J.L. Hardebeck, and G. Anderson. 2005. Constraints on fault slip rates of the southern Cali-

fornia plate boundary from GPS velocity and stress inversions. *Geophysical Journal International* 160: 634-50.

Burgmann, R., P.A. Rosen, and E.J. Fielding. 2000. Synthetic aperture radar interferometry to measure Earth's surface topography and its deformation. *Annual Review of Earth and Planetary Sciences* 28: 169-209.

Freed, A.M. 2005. Earthquake triggering by static, dynamic, and postseismic stress transfer. *Annual Review of Earth and Planetary Sciences* 33: 335-67.

Freed, A.M. 2007. Afterslip (and only afterslip) following the 2004 Parkfield, California, earthquake. *Geophysical Research Letters* 34: L06312, doi: 10.1029/2006GL029155.

Ji, C., K.M. Larson, Y. Tan, K.W. Hudnut, and K. Choi. 2004. Slip history of the 2003 San Simeon earthquake constrained by combining 1–Hz GPS, strong motion, and teleseismic data. *Geophysical Research Letters* 31: L17608, doi: 10.1029/2004GL020448.

Johanson, I.A. 2006. Slip characteristics of San Andreas fault transition zone segments, Ph.D. Thesis, University of California, Berkeley, 117 pp.

Johanson, I.A., E.J. Fielding, F. Rolandone, and R. Bürgmann. 2006. Coseismic and Postseismic Slip of the 2004 Parkfield Earthquake from Space-Geodetic Data. *Bulletin of the Seismological Society of America* 96(4b): S269-82.

Langbein, J., J.R. Murray, and H.A. Snyder. 2006. Coseismic and initial post-seismic deformation from the 2004 Parkfield, California, earthquake, observed by global positioning system, electronic distance meter, creepmeters, and borehole strainmeters. *Bulletin of the Seismological Society of America* 96: S304-20.

McCaffrey, R. 2004. DEFNODE User's Guide, Rensselaer Polytechnic Institute, Troy, 1995-2004. [http://www.rpi.edu/~mccafr/defnode/.]

McCaffrey, R. 2005. Block kinematics of the Pacific/North America plate boundary in the southwestern United States from inversion of GPS, seismological, and geologic data. *Journal of Geophysical Research* 110: B07401.

McCaffrey, R., A.I. Qamar, R.W. King, R. Wells, G. Khazaradze, C.A. Williams, C.W. Stevens, J.J. Vollick, and P.C. Zwick. 2007. Plate locking, block rotation and crustal deformation in the Pacific Northwest. *Geophysical Journal International*, doi: 10.1111/j.1365-264X.2007.03371.x.

Meade, B.J., and B.H. Hager. 2005. Block models of crustal motion in southern California constrained by GPS measurements. *Journal of Geophysical Research* 110: B03403.

Murray, J., and J. Langbein. 2006. Slip on the San Andreas fault at Parkfield, California, over two earthquake cycles, and the implications for seismic hazard. *Bulletin of the Seismological Society of America* 96: S283-303.

Okada, Y. 1985. Surface deformation due to shear and tensile faults in a half space. *Bulletin of the Seismological Society of America* 75: 1135-54.

Pearson, C. 2005. The National Spatial Reference System Readjustment of NAD 83. *Surveying and Land Information Science* 65: 69-74.

Savage, J. C. 1980. Dislocations in seismology. In: F.R.N. Nabarro (ed.), *Dislocations in solids*. Chapter 12, pp. 251-339. Amsterdam, Holland: North-Holland Publ. Co. 5 vols.

Segall, P., and J.L. Davis. 1997. GPS applications for geodynamics and earthquake studies. *Annual Review of Earth and Planetary Sciences* 25: 301-36.

Snay, R. 1999. Using the HTDP software to transform spatial coordinates across time and between reference frames. *Surveying and Land Information Systems* 59(1): 15-25.

Snay, R.A., and T. Soler. 2000. Part 2: The evolution of NAD 83. *Professional Surveyor* 20(2): 16-8.

Vorhauer, M.L. 2007. National readjustment of 2007. *The American Surveyor Magazine*, pages 48-54 (May 2007 issue).